 https://doi.org/10.3311/PPci.37771

Periodica Polytechnica Civil Engineering, 69(3), pp. 738–751, 2025

An Automated Method to Quickly Predict the Settlements of Embankments during Construction

Tao Liu[1], Baofeng Pan[1], Peng Yin[1*], Baiyi Chen[1], Hongxiang Tang[2]

[1] School of Infrastructure Engineering, Dalian University of Technology, Ling-gong Road 2., Ganjingzi District, 116024 Dalian, Liaoning Province, China
[2] State Key Laboratory of Coastal and Offshore Engineering, Dalian University of Technology, Ling-gong Road 2., Ganjingzi District, 116023 Dalian, Liaoning Province, China
[*] Corresponding author, e-mail: yp2021@mail.dlut.edu.cn

Received: 25 June 2024, Accepted: 24 March 2025, Published online: 09 April 2025

Abstract

In the process of embankment construction, the most significant point is the construction quality control, especially the settlement control. In order to predict the embankment settlement in the construction process quickly and conveniently, the automated modeling method is studied in this paper. A parametric model replicating the embankment building process was created using ABAQUS's built-in secondary development functionality. The model can consider multiple influencing factors to explore their effects on embankment settlement fully. The sensitivities demonstrated by each parameter were then evaluated to assess their effect on the total settlement. Based on these results, the SASLEF V1.0 program was created and granted software copyright certification. The developed software enables rapid analysis of the embankment layered filling process. The effectiveness of the software was verified by engineering cases. The study can provide a meaningful reference for embankment construction.

Keywords

embankment, settlement, parametric model, automated method, secondary development

1 Introduction

With the rapid development of the global economy, road construction, particularly the construction of highways, is advancing at an accelerated pace. Two significant challenges faced in highway construction are soft soil embankments and high fill embankments [1, 2]. Economically developed regions, especially coastal and riverbank areas, generally possess abundant soft soil resources. The level of infrastructure development in these areas is relatively high, particularly in the construction of highway networks [3]. However, the characteristics of soft soil, including high moisture content, low permeability, low natural strength, and high compressibility, can lead to excessive settlement of embankments when constructing roads on soft soil foundations [4, 5]. Furthermore, high fill embankments are widely used in the construction of mountainous roads, but their design and construction processes are relatively complex and often accompany significant settlement issues during the construction [6]. Therefore, in-depth research and solutions to these problems are crucial for enhancing the safety and durability of road construction [7–9].

Excessive settlement can lead to pavement cracks, road waterlogging, bridge head bumping, and other issues that can have a negative impact on highway safety and serviceability. Therefore, it is crucial to control embankment settlement during highway design and construction [10]. Embankment settlement occurs throughout the road's life cycle [11]. The percentage of settlement during the stages of pavement building, embankment construction, and highway operation is around 15%, 25%, and 60%, respectively [12]. The stage of embankment construction is when settlement is most great. Therefore, regulating embankment settlement during construction is essential to guaranteeing the quality of road building.

As a significant geotechnical issue, embankment settlement has attracted a lot of attention [13–19]. Methods commonly used to calculate embankment settlement include the layer-wise summation method (LSM), the empirical formulation method (EFM), and the finite element method (FEM). Among these methods, the FEM has been demonstrated to be an effective numerical tool for solving complex

Cite this article as: Liu, T., Pan, B., Yin, P., Chen, B., Tang, H. "An Automated Method to Quickly Predict the Settlements of Embankments during Construction", Periodica Polytechnica Civil Engineering, 69(3), pp. 738–751, 2025. https://doi.org/10.3311/PPci.37771

two- or three-dimensional settlement problems [20–22]. There have been several studies on embankment settlement on soft soil. Zhuang and Wang [18] investigated the deformation in highway pile-soil embankments subjected to moving vehicle loads based on FEM. Their findings revealed that the impact of pile spacing on settlement is more sensitive than the height of the embankment. They also found that the moving load increases the settlement of the embankment. Jia et al. [23] studied a technique for predicting embankment settlement that is impacted by the relationship between soil consolidation and traffic load. A soft soil embankment roadway under soil consolidation was modeled using finite elements to forecast the long-term settlement caused by the interaction of soil consolidation and traffic loads. According to the findings, natural soft soil consolidation is the primary cause of the settlement. Pham and Dias [24] conducted a parametric study on the performance of geosynthetic-reinforced and pile-supported (GRPS) embankments using a three-dimensional numerical analysis method. The effects of fill embankment height, geosynthetic stiffness, modified area ratio, subsoil stiffness, friction angle, and fill cohesion were investigated. Numerical analyses of cohesive and non-cohesive embankment soils were conducted to emphasize the effect of fill cohesion on the load transfer mechanism of GRPS embankments. The numerical results show that the GRPS system exhibits better performance in reducing embankment settlement. Current research on the prediction of embankment settlement mainly focuses on post-construction settlement, while little research has been done on the prediction of settlement during embankment construction.

In this study, a parametric model for simulating deformation during embankment construction is developed. The Duncan-Chang model was used to capture the complexities of soil behavior. Subsequently, a parametric model is generated employing the built-in secondary development tool of ABAQUS finite element software [25] to replicate the embankment construction process. The model can completely study the impact of several influencing factors on embankment settlement. The sensitivity of each influencing factor is then analyzed, revealing their different roles in the overall framework. In addition, one of the results of this research is the implementation of SASLEF V1.0 software [26], an innovative embankment settlement analysis software. SASLEF V1.0 software [26] has received due recognition through software copyright certification, proving its pioneering nature. In order to verify its effectiveness, the software is validated against real engineering cases to confirm its reliability and applicability in real scenarios.

2 Parameterization of embankment models

2.1 Description of the problem

The embankment settlement consists of two parts, one is the underlying foundation settlement, and the other is the embankment fill itself. The geometry of the numerical models is shown in Fig. 1. According to the specifications [27], the filling height of the embankment will not exceed 20 m, usually. The geometric form of the embankments will vary with the height of the embankment. When the filling height is less than 12 m, the geometric model of the embankment is Model A, as shown in Fig. 1 (a). When the height of the fill exceeds 12 m but does not exceed 20 m, the stepped embankment must be used. The embankment form is Model B, as shown in Fig. 1 (c). The embankment settlement problem is a plane strain problem. In the analysis, only one of the cross-sections needs to be analyzed. Thus, the three-dimensional model is converted into a two-dimensional model, as shown in Fig. 1 (b) and Fig. 1 (d). This was a reasonable assumption for the present study.

2.2 Parameterization for the model

Although the model has been simplified, it is still cumbersome to model when the fill height, fill slope, grade-by-grade fill thickness, and material parameters change. Therefore, the models are parameterized, as shown in Fig. 2.

In Fig. 2 (a), *AA'B'B* represents the underlying foundation and *CC'D'D* is the embankment. In Fig. 2 (b), *AA'B'B* represents the underlying foundation, *CC'D'D* and *EE'F'F* are the embankment, and *DE* and *D'E'* are berm roads.

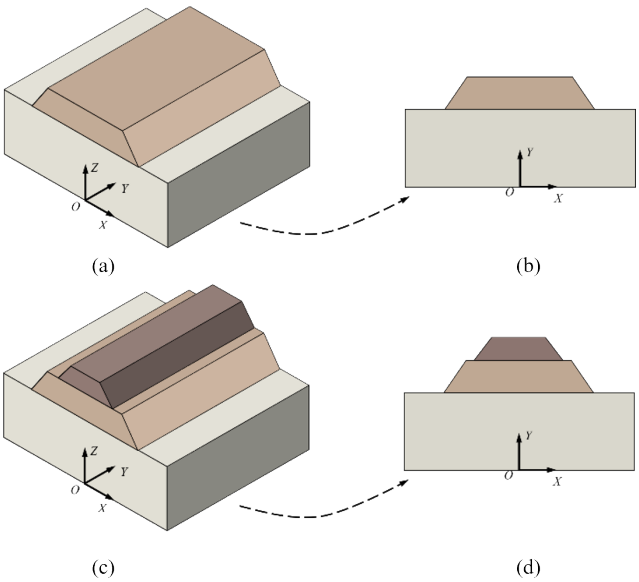

Fig. 1 The geometry of the numerical models; (a) Model A; (b) plane strain model of Model A; (c) Model B; (d) plane strain model of Model B

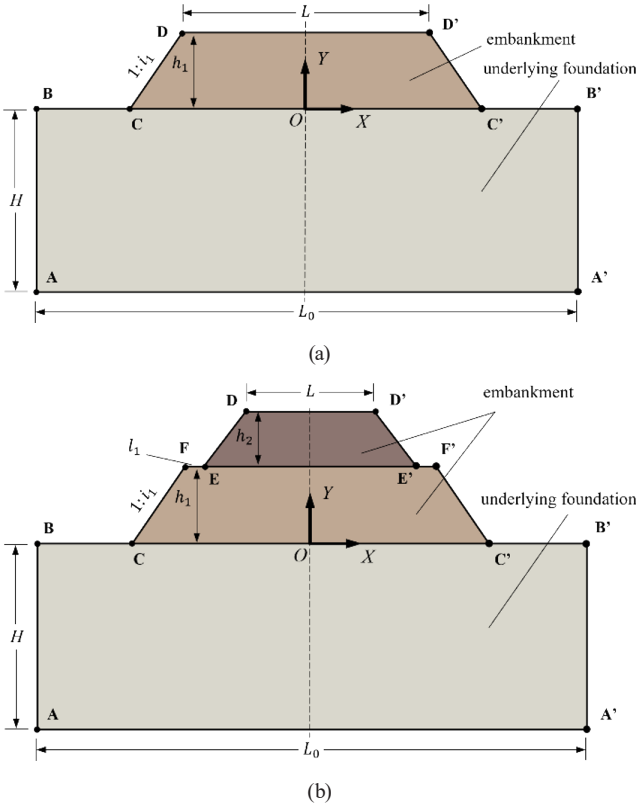

Fig. 2 Parametric model; (a) Model A; (b) Model B

Taking the symmetry axis of the model as the y-axis and the top surface of underlying foundation as the x-axis to establish a Cartesian coordinate system, then points *ABCDEF* and *A'B'C'D'E'F'* are symmetric about the y-axis, and the coordinates can be obtained as shown in Table 1.

In Table 1 L_0 is the width of the underlying foundation, H is the depth of the underlying foundation, L is the crest width, h_1 is the filling height of the first embankment step, $1:i_1$ (V:H) is the slope of the first embankment step, h_2 is the filling height of the second step, $1:i_2$ is the slope of the second embankment step, l_1 is the width of the berm road.

3 Finite element simulation of embankments

3.1 Duncan-Chang EB constitutive model

There are several constitutive models that can be used to capture the stress-strain behavior of soils. The choice of one constitutive model over another is determined by a variety of criteria, including the issue to be solved, the parameters needed, and the kind of soil being represented. The non-linear elastic behavior of soil can be reflected by the Duncan-Chang EB constitutive model [28].

In 1963, Kondner [29] proposed the following stress-strain equation based on the hyperbolic stress-strain relationship curves of triaxial tests on a large number of soils, as follows in Eq. (1):

Table 1 Coordinates of each point at the parameterized model

Type	Model A	Model B
A	$\left(-\frac{L_0}{2},-H\right)$	$\left(-\frac{L_0}{2},-H\right)$
B	$\left(-\frac{L_0}{2},0\right)$	$\left(-\frac{L_0}{2},0\right)$
C	$\left(-\left(\frac{L}{2}+i_1\times h_1\right),0\right)$	$\left(-\left(\frac{L}{2}+i_2\times h_2+l_1+i_1\times h_1\right),0\right)$
D	$\left(-\frac{L}{2},h_1\right)$	$\left(-\frac{L}{2},h_1+h_2\right)$
E	–	$\left(-\left(\frac{L}{2}+i_2\times h_2\right),h_1\right)$
F	–	$\left(-\left(\frac{L}{2}+i_2\times h_2+l_1\right),h_1\right)$
A'	$\left(-\frac{L_0}{2},-H\right)$	$\left(-\frac{L_0}{2},-H\right)$
B'	$\left(-\frac{L_0}{2},0\right)$	$\left(-\frac{L_0}{2},0\right)$
C'	$\left(\frac{L}{2}+i_1\times h_1,0\right)$	$\left(\frac{L}{2}+i_2\times h_2+l_1+i_1\times h_1,0\right)$
D'	$\left(-\frac{L}{2},h_1\right)$	$\left(-\frac{L}{2},h_1+h_2\right)$
E'	–	$\left(-\left(\frac{L}{2}+i_2\times h_2\right),h_1\right)$
F'	–	$\left(-\left(\frac{L}{2}+i_2\times h_2+l_1\right),h_1\right)$

$$\sigma_1-\sigma_3=\frac{\varepsilon_1}{a+b\varepsilon_1}, \tag{1}$$

where a and b are model constants. Later, Duncan and Chang [28] proposed the Duncan-Chang constitutive model, which is now widely used and based on this hyperbola.

The Duncan-Chang EB constitutive model is a tangential model. In order to reflect the nonlinearity of soil deformation, the tangential Young's modulus E_t and the tangential bulk modulus B_t are used in this model, and their expressions are as follows:

$$E_t=Kp_a\left(\frac{\sigma_3}{p_a}\right)^n\left[1-\frac{R_f\left(\sigma_1-\sigma_3\right)\left(1-\sin\varphi\right)}{2c\cos\varphi+2\sigma_3\sin\varphi}\right]^2, \tag{2}$$

$$B_t=K_bp_a\left(\frac{\sigma_3}{p_a}\right)^m, \tag{3}$$

where K and K_b are modulus numbers, n and m are modulus exponents, which can be obtained experimentally; p_a is the atmospheric pressure; σ_1 and σ_3 are the maximum and minimum principal stresses; R_f is the damage ratio, which is defined as the ratio of the ultimate partial stress to the strength of the soil; c and φ are the cohesion and the internal friction angle of the soil, respectively.

In unloading-reloading, the Duncan-Chang model uses the unloading-reloading modulus to describe the elastic theory, and its equation is shown in Eq. (4):

$$E_{ur} = K_{ur} p_a \left(\frac{\sigma_3}{p_a} \right)^n, \tag{4}$$

where K_{ur} is modulus number for unloading, which can be obtained experimentally; the parameter n can be equal to n in Eq. (2).

3.2 Load and boundary conditions

When calculating embankment deformation, it is usually assumed that the embankment is constructed once to the top and the soil load is applied at once, in this case, each part of the load is borne by the whole structure. In fact, the embankment is filled layer by layer. When the construction reaches a certain height, only the filled soil below that height will bear this part of the load. There is no effect on the upper layer of soil that has not yet been filled, and the upper layer is not affected by the lower layer of soil [30]. The difference in the deformation mechanism between layer-by-layer loading and one-time loading makes the deformation calculation results different. The calculation method using one-time loading cannot truly simulate the condition of embankment under layer-by-layer filling. Therefore, the self-weight of the embankment fill is applied layer by layer. To ensure sufficient compaction, the thickness d of each layer is generally no more than 0.3 m. In this paper, 0.25 m was considered.

The pre-consolidation pressure always has an important influence on the embankment settlement [31]. In the modeling process, it was considered that the underlying foundation had already achieved settlement equilibrium by self-weight long before the embankment construction. Thus, the settlement of the underlying foundation was only affected by the gravity of the embankment fill. For the newly filled embankment, the compaction stress of each layer is the pre-consolidation pressure. For the underlying foundation, the pre-consolidation pressure is related to the geological history conditions which can be measured by the Casagrande method [32].

There are two types of boundary conditions traditionally required for embankment settlement, displacement and pore pressure [33]. When displacement boundaries are applied, there must be sufficient distance to eliminate the effect of boundary conditions on the finite element analysis results. Therefore, a sensitivity analysis was developed to determine the appropriate underlying foundation width L_0 to maintain the finite element results accurately as well as minimize the time of calculation. Through the calculation for Models A and B, when the underlying foundation width L_0 was taken as 150 m and 200 m respectively, the influence of the underlying foundation width on the calculation results was negligible. Taking Model A as an example, it is analyzed as shown in Fig. 3. As the model width increases, the settlement of the embankment is stabilizing, which is mainly due to the weakening of the influence of the boundary, and is basically stable when the model width is 150 m. Therefore, this value is chosen as the modeling width, the underlying foundation width of Model A was taken as 150 m and 200 m for Model B.

Three boundary conditions were considered in this paper, as shown in Eq. (5). Along the left and right boundaries of the underlying foundation, it was assumed that the soil moves only in the vertical direction. The movement of the bottom surface at the underlying foundation was limited both horizontally and vertically since a basement rock layer was assumed to be present here:

$$\left.\begin{array}{l} x = -\dfrac{L_0}{2}, x = \dfrac{L_0}{2} : u = 0 \\ y = -H : u = 0, v = 0 \end{array}\right\}. \tag{5}$$

3.3 Element type and size

The soil is a porous structure, and its voids can be occupied by air and water. The element type used to divide the model was a plane-strained, four-node quadrilateral element with bi-directional displacement (ABAQUS element code: CPE4). Since the models cannot be calculated properly with the hourglass phenomenon when using the CPE4R element [33].

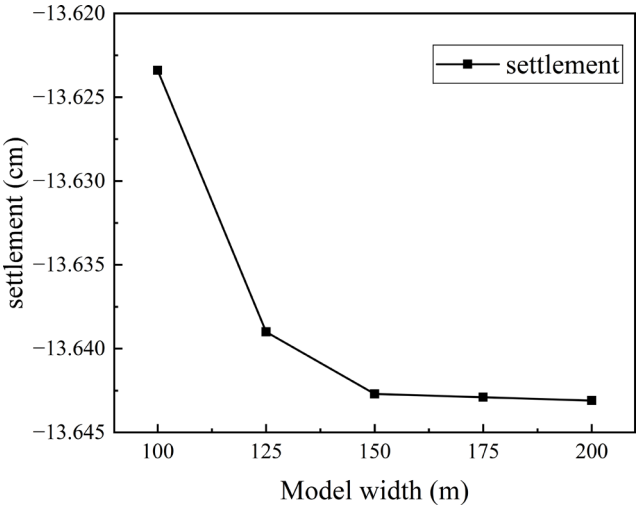

Fig. 3 Relationship between model width and maximum settlement values

A sensitivity analysis was developed to determine the appropriate suitable element sizes to maintain the FEM results accurate as well as minimize the time of calculation. This was realized by observing the differential embankment settlement while the element sizes varied. A uniform element size was applied throughout the model. Eventually, it was discovered that the differential embankment settlement was nearly steady when the element size was 0.50 m × 0.50 m or less, and hence, this element size was applied in this research. It can be seen from Fig. 4 that as the cell size increases, the change in the settlement calculation value increases and stabilizes when the cell size is less than 0.5 m. This is because the smaller the cell size, the more accurate the calculation. Therefore, the cell size can be taken as 0.5 × 0.5 m.

3.4 Parameters for the model

A comprehensive literature review was conducted to select the material properties and geometry for the numerical model. The geometry parameters of the numerical models are shown in Table 2. Model A is a 6 m height symmetric embankment, with a 30 m road width and 1:1.45 (V:H) inclined slopes. The foundation is a 10 m thick saturated clay layer lying on a bedrock layer. The Model B is a stepped embankment, with a 30 m road width. The first step is 6 m high, with a 1:1.45 inclined slope, and the second step is also 6 m high, with a 1:1.25 inclined slope. The foundation is a 10 m thick saturated clay layer lying on a bedrock layer. In particular, the choice of model depth for the absence of bedrock is an issue worth investigating, and it is generally accepted that the model depth can be taken at depth where the stress increment decreases below 20% of overburden effective stress [34–36].

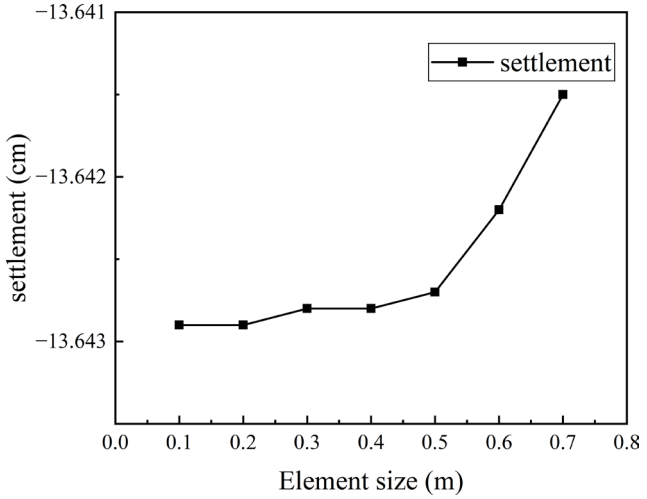

Fig. 4 Relationship between element size and maximum settlement values

The properties of the embankment fill and the underlying foundation play an essential role in the embankment settlement study. In this study, soil properties from the test results reported by other researchers were used. Two different soil zones were considered in this study; the embankment fill and the underlying foundation soil. For this purpose, the embankment fill was selected to be limestone clay, and the underlying foundation soil was considered to be clay. The constitutive relations of both the embankment fill and underlying foundation soil were simulated by the Duncan-Chang EB model [37, 38] with the parameters indicated in Table 3. Table 3 also shows the pre-consolidation pressure p_c.

In the models, the acceleration of gravity g is 9.8 N/kg, the density of the embankment fill is 1.996 g/cm^3, and the density of the underlying foundation soil is 2.177 g/cm^3.

3.5 Automated modeling of finite element models

Due to the nonlinearity of the geotechnical constitutive and the complexity of loading and boundary conditions, it is very difficult to solve the geotechnical engineering problems by analytical methods. Therefore, numerical calculations are usually required. The nonlinear constitutive of the material in the calculation could be truly reflected and the analysis of complex boundary conditions could be realized by FEM. ABAQUS is a powerful general-purpose finite element software [25], especially in solving nonlinear problems with good applicability. With the change in the filling height and slope of the embankment, it will be very tedious to recreate the model. To make the FEM more widely used in road engineering, it is necessary to realize automated modeling. Therefore, the secondary development function of ABAQUS software [25] was used.

The ABAQUS provides many library functions to the developer through Python. These library functions are called through the Python language to enhance ABAQUS interactive operations. This allows users to bypass the ABAQUS interface and directly manipulate the ABAQUS kernel for modeling, meshing, specifying material properties, submitting jobs, post-processing analysis results, etc. It avoids the completely manual operation in the pre-processing process using ABAQUS, saving a lot of time and effort and improving work efficiency. In this paper, the pre-processing and post-processing of the model were completed in Python language. Meanwhile, the Duncan-Chang constitutive model was extended through the user-define material subroutine (UMAT) in ABAQUS/Standard [25] to address the behavior of soil. The UMAT subroutine was

Table 2 Geometric parameter values of the model

Parameters	L_0/m	d/m	H/m	L/m	h_1/m	i_1	h_2/m	i_2	l_1/m
Model A	150	0.25	10	30	6	1.45	–	–	–
Model B	200	0.25	10	30	6	1.45	6	1.25	2

Table 3 Duncan-Chang constitutive model parameters

Parameters	K	p_a/kPa	n	R_f	c/kPa	φ/(°)	K_{ur}	K_B	m	p_c
Embankment	300	101.3	0.4	0.6	84.3	27.3	690	200.0	0.5	338.8
Underlying foundation	400	101.3	0.3	0.75	35.4	17.2	400	100.0	0.5	100.0

written in Fortran language and could be called by Python files [39, 40]. These Python script files can be read directly by the ABAQUS command and then generate an input file (.inp), which is submitted and run in ABAQUS to obtain a result file (.dat). And the required data results can be read from the result files. The whole automated modeling process is shown in Fig. 5. The modeling process is similar to that of modeling with ABAQUS.

Two two-dimensional FEM models were established, using commercial software-ABAQUS [25]. A series of geometry and material parameters can be modified in the Python program to establish the model, resulting in enabling the prediction of construction conditions. Considering the actual construction process of layer-by-layer compaction, the embankment model was divided according to the actual thickness of each layer d. Through the birth-death element function provided by ABAQUS, each layer of fill was advanced deactivated, and then reactivated step by step, thus activating all material parameters and geometric models of that layer into the analysis step. In this way, the ABAQUS model is used to establish and simulate the layer-by-layer filling process of embankment. A partial enlargement of the model is shown in Fig. 6.

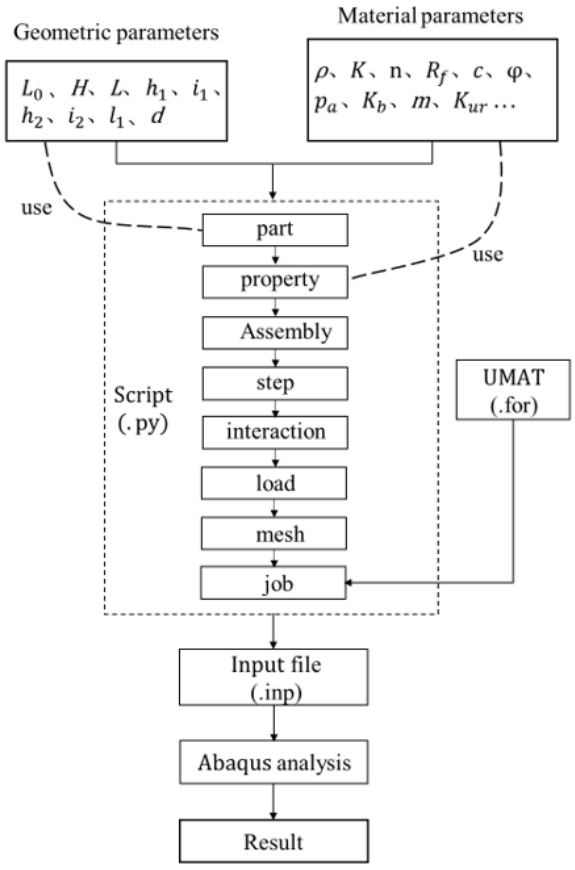

Fig. 5 Automated modeling process

4 Results and sensitivity analysis

4.1 FEM Results

Fig. 7 shows the deformed contour of the Model A settlement during construction. The embankment settlement distribution can be seen as the construction height changes. Embankment settlement increases with increasing construction height. The maximum embankment settlement value is 0.1412 m at the upper of the underlying foundation. Model B results can be seen in Fig. 8. For Model B, the first construction step is similar to Model A, therefore only the second step is shown. The maximum settlement always occurs near the upper of the underlying foundation. During construction, there are important upward vertical movements near the foot. This is consistent with what other researchers have found [41].

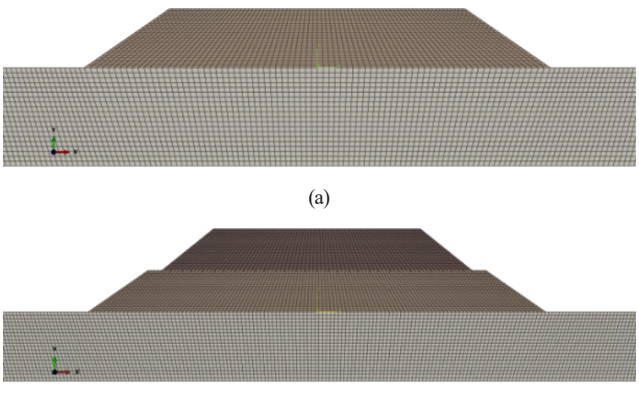

(a)

(b)

Fig. 6 ABAQUS automatic modeling; (a) Model A; (b) Model B

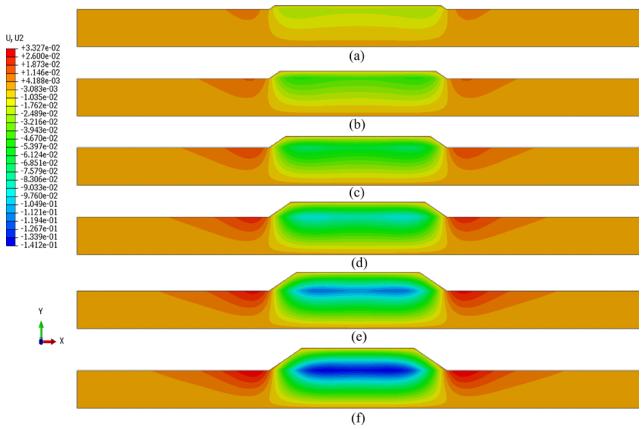

Fig. 7 Embankment settlement of Model A during construction (a) 1 m; (b) 2 m; (c) 3 m; (d) 4 m; (e) 5 m; (f) 6 m height embankment

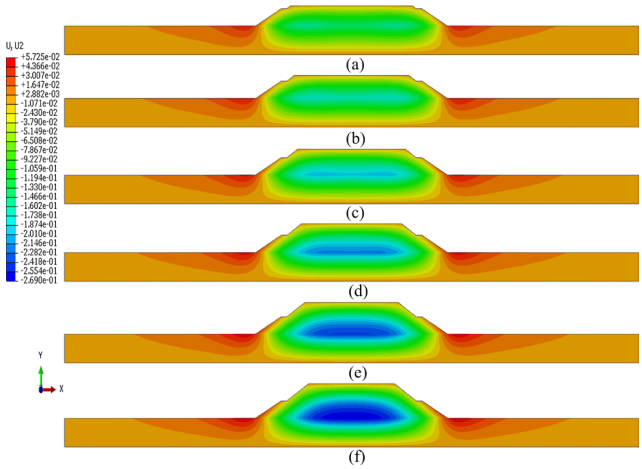

Fig. 8 Embankment settlement of Model B during construction (a) 7 m; (b) 8 m; (c) 9 m; (d) 10 m; (e) 11 m; (f) 12 m height embankment

For the end of construction, Fig. 9 shows the settlements at the embankment base and the horizontal displacements at slop feet. As expected, horizontal displacements are outwards. From Fig. 9, with the increase of embankment construction height layer by layer, the horizontal displacement at the embankment foot and the maximum embankment settlements are increasing with a very similar linear growth trend. These are consistent with the previous research [42]. The maximum embankment settlement always occurs near the top of the underlying foundation. The horizontal position of the maximum embankment settlement is constantly changing. The distance from the symmetry line decreases with the increase of the embankment construction height and is constantly approaching the symmetry line. In Model B, when the fill height reaches 11 m, the maximum settlement position reaches the symmetry line of the embankment, after that, the position remains the same, but the value of settlement

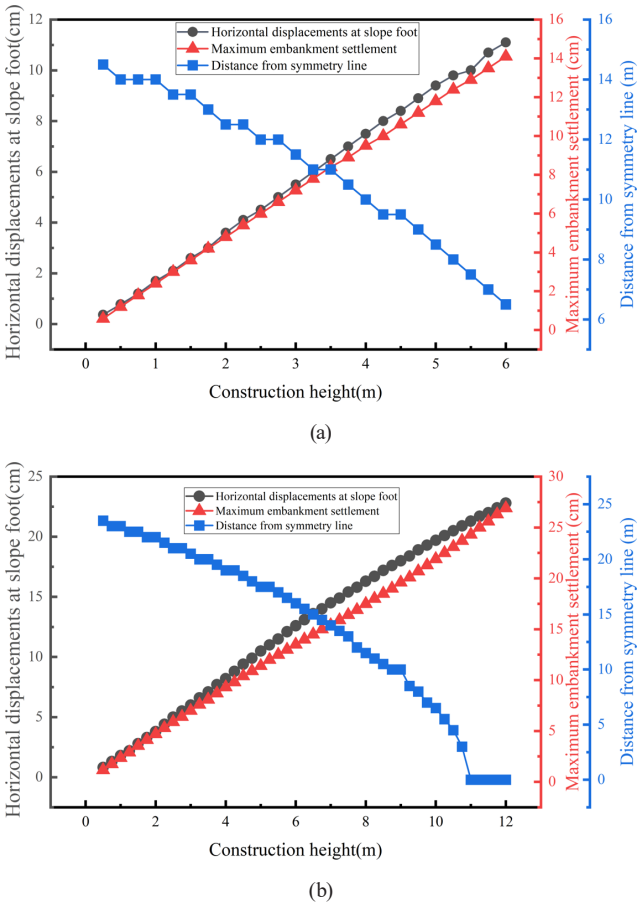

Fig. 9 Deformation of embankment with different embankment construction heights (a) Model A; (b) Model B

keeps increasing. This is probably because the width of the upper layer fill decreases as the construction progresses.

4.2 Sensitivity analysis

The most difficult problem in geotechnical analysis and calculation is how to determine the geotechnical model parameters reasonably. There are many parameters in Model A and Model B, which affect the embankment settlement in varying degrees. The purpose of the parameter sensitivity study is to identify sensitive parameters and identify critical parameters that significantly impact embankment settlement.

In the parametric study, some of the design considerations and potential problems that can be expected during and after the construction of the embankment are discussed. The Morris screening method (MSM) is a widely used sensitivity analysis method in various fields, currently. MSM varies one of the model parameters x_i at a time within the range of variable values, the other parameter values are fixed. Then, MSM runs the model to obtain the

result of the objective function $y(x) = y(x_1, x_2, x_3, \ldots, x_n)$, and uses the influence value e_i to determine the degree of influence of parameter changes on the output values [43], as shown in Eq. (6):

$$e_i = \frac{y^* - y}{\Delta_i}, \tag{6}$$

where y^* is the output value after parameter change; y is the output value before parameter change; Δ_i is the parameter change amplitude.

It is shown that relatively high computational accuracy is obtained when each parameter is varied in a fixed step over a range of variation. Hence, the modified MSM [44] first selects an initial value in the parameters range, and then selects multiple input data with fixed steps of variation, and the sensitivity discriminant S takes the averages of multiple MSM values. Its equation is shown in Eq. (7):

$$S = \sum_{i=0}^{n-1} \frac{\left(Y_{i+1} - Y_i\right)/Y_0}{\left(P_{i+1} - P_i\right)/100} \Big/ (n-1), \tag{7}$$

where S is the sensitivity discriminant; Y_i is the output value of the th change of the parameter; Y_{i+1} is the output value of the $(i + 1)^{\text{th}}$ change of the parameter; Y_0 is the initial value of the selected parameter; P_i is the change rate of the ith value of the parameter under study about the initial value; P_{i+1} is the change rate of the $(i + 1)^{\text{th}}$ value of the parameter under study about the initial value; n is the times of parameter changes.

For Model A and Model B, the sensitivity analysis results of the maximum settlement during construction were quantified by using the modified MSM. The value of a model parameter was changed in a fixed step size of 5% by taking from −20% to 20% respectively, while the other relevant parameter values were kept constant. Among the model parameters, all of them were investigated except for L_0, g and p_a.

To evaluate the sensitivity of the model parameters better, the sensitivity was divided into four levels as shown in Table 4 [45], where S_i is the sensitivity of the i^{th} parameter.

Due to a large number of models to be analysis during the investigation, Python script files were used. The results of sensitivity analysis are given in Table 5 and Fig. 10.

The positive reaction means that as the value of the parameter increases, the target value becomes larger; the negative reaction means that as the value of the parameter increases, the target value decreases.

From Table 5 and Fig. 10, it can be seen that for both Model A and Model B, the index of d is 0.01 with class I, and the influence of the layer-by-layer filling thickness d on embankment settlement is negligible with guaranteed compaction. The sensitivity for the crest width L is negative, indicating that the embankment settlement decreases as L increases. However, the reactions of the underlying foundation and the new filling embankment on settlement are different. Here, L_j is used to evaluate the settlement sensitivity of different embankment parts, and its formula is shown in Eq. (8):

$$L_j = \sum_{i=1}^{n} \left|S_{ji}\right|, \tag{8}$$

where S_{ji} is the i^{th} part sensitivity of embankment. The results are shown in Table 6.

Table 4 Sensitivity class

Class	Index	Sensitivity
I	$0 \le \lvert S_i \rvert < 0.05$	Small to negligible
II	$0.05 \le \lvert S_i \rvert < 0.2$	Medium
III	$0.2 \le \lvert S_i \rvert < 1$	High
IV	$\lvert S_i \rvert \ge 1$	Very high

Table 5 Results of sensitivity analysis on parameters

Parameters	Model A		Model B	
	Index	Class	Index	Class
d	0.01	I	0.01	I
L	−0.19	II	−0.16	II
H	1.22	IV	1.23	IV
K	−0.51	III	−0.43	III
n	0.24	III	0.21	III
R_f	0.97	III	0.91	III
K_b	−0.50	III	−0.57	III
p_c	−0.40	III	−0.41	III
h_1	0.93	III	0.45	III
i_1	−0.07	II	−0.02	I
l_1	–	I	−0.01	I
ρ_1	1.00	IV	0.44	III
K_1	−0.04	II	−0.06	II
n_1	−0.02	I	−0.03	I
R_{f1}	0.10	II	0.15	II
K_{b1}	0.00	I	0.01	I
p_{c1}	−0.01	I	−0.02	I
h_2	–	–	0.48	III
i_2	–	–	−0.07	II
ρ_2	–	–	0.56	III
K_2	–	–	0.01	I
R_{f2}	–	–	−0.03	I

Notes: reaction of the model:
Positive
Negative
I: Small to negligible, II: medium, III: high, IV: very high

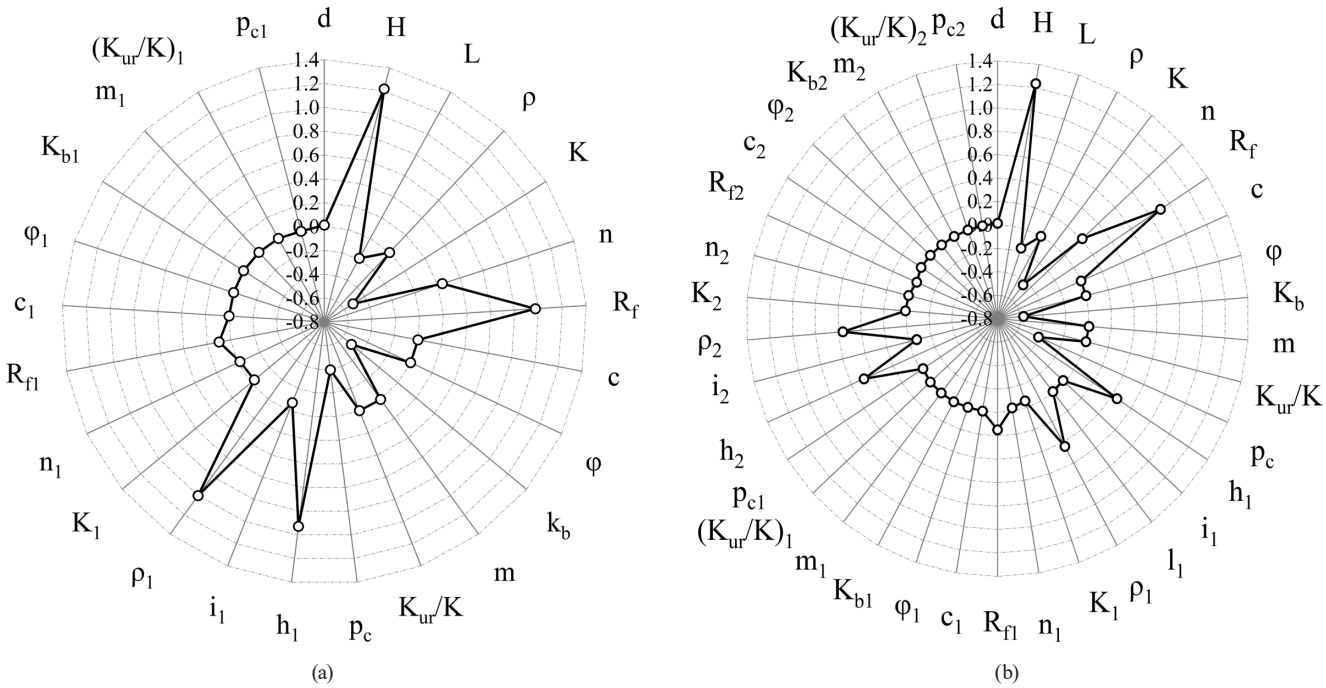

Fig. 10 Sensitivity parameter distribution; (a) Model A; (b) Model B

Table 6 The settlement sensitivity of each embankment part

Degree of influence	Underlying foundation	The first step	The second step
Model A	3.85	2.17	–
Model B	3.77	1.18	1.16

In Table 6, the settlement sensitivity of underlying foundation in Model A and Model B is much greater than embankment. It means that the underlying foundation has a greater influence on embankment settlement.

In Table 6, the settlement sensitivity of underlying foundation in Model A and Model B is much greater than embankment. It means that the underlying foundation has a greater influence on embankment settlement.

Among the underlying foundation parameters, it can be seen that for both Model A and Model B, the depth H of the underlying foundation has the greatest influence, with sensitivity values of 1.22 and 1.23, respectively. As expected, H has a positive reaction on the settlement; modulus number K and K_b, modulus exponent n, failure ratio R_f and the pre-consolidation pressure p_c, all have a large reaction on Model A and Model B settlement, where n and R_f are positive and K, K_b and p_c are negative. The contribution of cohesion c and internal friction angle φ of both Model A and Model B settlement is negligible in all soil layers. When the soil strength is small, the significant development of plastic deformation will lead to an increase in settlement [46]. The c and φ are the most important factors affecting the plastic deformation. The sensitivity parameters of density ρ, modulus exponent m and modulus number for unloading K_{ur} of the underlying foundation are zero, which is due to the fact that the embankment construction is a loading process independent of the unloading factor.

For embankment fill, the height h and the density ρ of the fill have a large reaction on Model A and Model B settlement with a sensitivity of III and positive reaction. Thus, avoiding high-fill embankments and using lightweight materials can effectively reduce construction settlement. The embankment slope rate 1:i has a negative reaction on both Model A and Model B embankment settlements. This is because the steeper the slope of the embankment, the less fill is required on both sides of the embankment. Modulus number K and failure ratio R_f have positive and negative effects on embankment settlement, respectively. R_f is numerically larger and more sensitive than that of K, therefore it is important to accurately determine the R_f for the prediction of settlement. However, in Model B, R_f of the second layer of fill shows a minimal negative reaction.

In addition, the embankment settlement is almost not affected by the compaction stress p_c, when the fill is guaranteed to be compacted. The reaction of ramp width on embankment settlement is also negligible.

5 Establishment of analysis software

A graphical user interface (GUI) was carefully designed using the advanced functions that are included into ABAQUS, utilizing the theoretical foundations previously explained. A custom software package is the result of this effort, as shown graphically in Fig. 11. The software, also known as SASLEF V1.0 software [26], makes it easier to perform a thorough visual modeling study. A user-friendly interface provided by SASLEF V1.0 software [26] enables straightforward interaction with the complexities of modeling. Notably, this novel program has successfully applied for and obtained a software copyright certificate in China, demonstrating its originality and intellectual integrity. The development of the software will contribute to the rapid analysis of settlement during embankment design and construction.

As shown in Fig. 11, the interface consists of three parts: an embankment schematic diagram, a parameters input box, and a Duncan-Chang EB model input box, each with default values set for the parameter boxes:

1. Embankment schematic diagram: users can fill in relevant parameters based on this diagram.
2. Parameters input box: responsible for inputting the embankment model number, geometric parameters, layering fill thickness, etc.
3. Duncan-Chang EB model input box: responsible for inputting the Duncan-Chang EB model for the original foundation and the newly filled embankment.

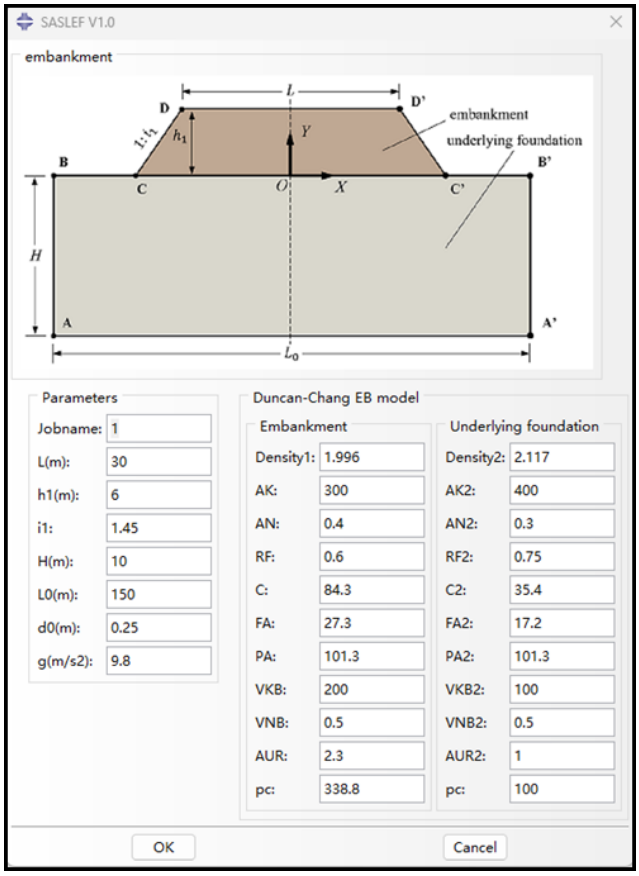

Fig. 11 SASLEF V1.0 software

SASLEF V1.0 software usage flowchart is shown in Fig. 12. When calculating embankment settlement, sequentially enter the parameters in the main interface as shown in Fig. 11, and after completing, click 'OK'. The software will automatically execute calculations, and you will need to wait a few minutes to obtain the final calculation results.

6 Software verification

6.1 Embankment above soft soil

In order to verify the effectiveness of the developed software, two real cases were used for verification.

1. Case 1:
   In order to verify the effectiveness of the developed software, the Dalian Jinpu Line project is used as an example [47, 48]. Because of the complexity of this project, it needs to be simplified. For analytical purposes, the simplified embankment is divided into two different layers. The underlying foundation, which was 15 m deep, was a compacted clay layer, while the embankment, which was 2 m high, was a lime-stabilized soil composition. Three settlement observation points were set up, with C-1 being the left foot of the slope, C-2 being the center point, and C-3 being the right foot of the slope. The observation of settlement was done by means of settlement boards.

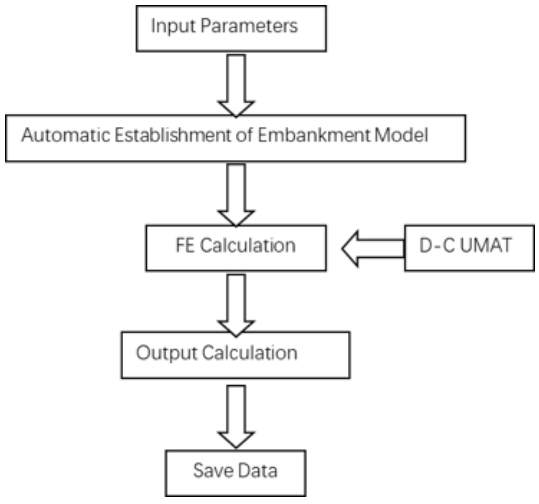

Fig. 12 SASLEF V1.0 software usage flowchart

As seen in Fig. 13, the embankment's geometric characteristics showed up as a structure that was 12.4 m wide at the top and 18.4 m wide at the bottom, with a slope of 1:1.5. In order to provide a thorough examination, Table 7 lists the precise parameters that define all layers in the embankment. The application and accuracy of the established model in the face of complicated engineering situations are confirmed by this thorough analysis of the Dalian Jinpu Line Project, which acts as a useful evaluation.

Rapid analysis was performed using the developed SASLEF V1.0 software [26] and result was shown in Fig. 14. The model monitoring points were arranged at the left and right feet of the embankment and at the center. In comparison with the measured data, the results are shown in Fig. 14. The numerical calculation results of the settlement are slightly larger than the measured results, and the maximum difference is not more than 21%. The comparison results are more consistent with the measured results, which proves the effectiveness of SASLEF V1.0 software [26].

2. Case 2:

On a certain highway in Hangzhou, the road width is 26 m, the fill height is 5.2 m, and the slope is 1:1.5, as shown in Fig. 15. During the filling process, the settlement at the center point of the embankment, C-1, was monitored. The underlying foundation consists of a clay layer, which is 25 m deep. Table 8 lists the parameters that define all layers in the embankment. The observation of settlement was done by means of settlement boards.

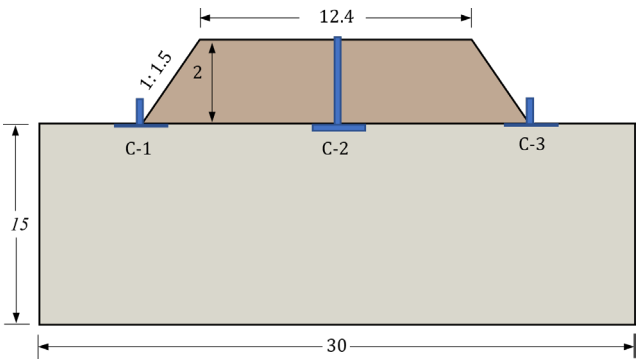

Fig. 13 Embankment model of Jinpu Line Project

Using the SASLEF V1.0 software [26] proposed in this article, rapid modeling and analysis were conducted for this case. According to the finite element simulation results, the observed settlement of the embankment was 13.96 cm, while the predicted result was 15.82 cm. The predicted result is 13.3% higher than the measured value, showing good agreement between the predicted and observed results.

6.2 Embankment above soft soil with vertical drain

On a certain highway in Ningbo, the road width is 30 m, the fill height is 2.4 m, and the slope is 1:1.5, as shown in Fig. 16. During the filling process, the settlement at the center point of the embankment, C-1, was monitored. The underlying foundation consists of a clay layer, which is 30 m deep, with a permeability coefficient of $k = 10 \times 10^{-5}$ m/d, as shown in Fig. 16. Table 9 lists the parameters that define all layers in the embankment. The observation of settlement was done by means of settlement boards.

According to the SASLEF V1.0 software [26] simulation results, the observed settlement of the embankment was 6.6 cm, while the predicted result was 7.3 cm. The predicted result is 10% higher than the measured value, indicating a good agreement between the predicted and observed results, which demonstrates the effectiveness of the prediction method.

The software developed in this research has taken into account the influence of factors such as the soil properties and the embankment section form. It is able to quickly analyze the settlement during the layered construction of embankment, which is fast, visualized, and easy to operate. However, the software still has some shortcomings. For example, it is not possible to analyze the effect of complex foundation treatment methods on settlement, including geogrids and cement mixing piles. Nevertheless, the user can adopt the consideration of the reinforced zone as a composite soil foundation [49].

7 Conclusions

The main purpose of this study is to make a reasonable prediction of the settlement in the embankment construction process. The embankment construction process was

Table 7 Duncan-Chang constitutive model parameters of Jinpu line

Parameters	K	p_a/kPa	n	R_f	c/kPa	φ/(°)	K_{ur}	K_B	m	p_c
Lime soil	303.76	101.3	0.3715	0.72	221.46	17	759.39	24.35	0.2156	338.8
Silty clay	280	101.3	0.6817	0.8457	29.72	16	179.5	19.03	0.3543	100.0

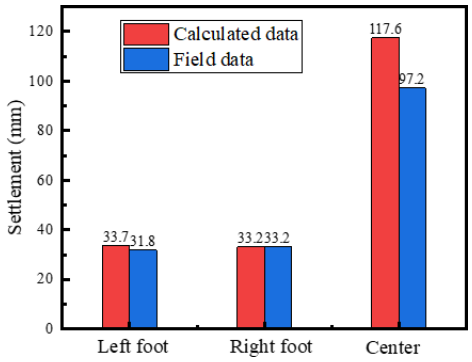

Fig. 14 Comparison of calculated and measured results

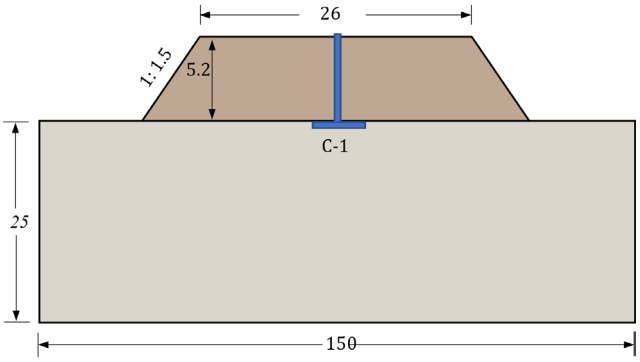

Fig. 15 Embankment model of Hangzhou highway

Table 8 Duncan-Chang constitutive model parameters of Hangzhou highway

Parameters	K	p_a/kPa	n	R_f	c/kPa	φ/(°)	K_{ur}	K_B	m	p_c
Filler	185	101.3	0.43	0.76	31.3	28.3	239	20.5	0.25	338.8
Foundation	106	101.3	0.54	0.86	39.5	16.8	168	17.3	0.38	100.0

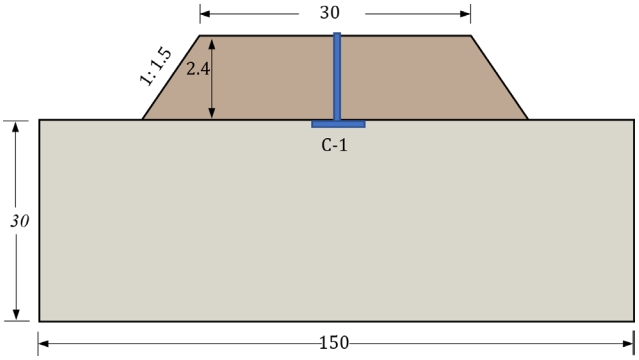

Fig. 16 Embankment model of Ningbo highway

Table 9 Duncan-Chang constitutive model parameters of Ningbo highway

Parameters	K	p_a/kPa	n	R_f	c/kPa	φ/(°)	K_{ur}	K_B	m	p_c
Filler	170	101.3	0.41	0.83	30.0	28.5	300	22.3	0.25	338.8
Foundation	213	101.3	0.43	0.86	30.5	14.7	364	15.1	0.33	100.0

parametrically modeled using the secondary development function in ABAQUS finite element software [25]. By establishing a number of parameters, the model was programmed to take into account the impact of different factors on settlement. These influencing factors can be varied by changing the parameters. The sensitivity of each impacting component was then examined in order to offer a guide for enhancing embankment building and design methods. This research work led to the development of the SASLEF V1.0 software [26], which encapsulates the parametric model. SASLEF V1.0 software [26] has been certified as a software copyright. Finally, 3 real engineering case study was used to validate the software and demonstrate its usefulness and reliability. The limitations of the software are also discussed in this paper.

Acknowledgement
The research was supported by National Natural Science Foundation of China (No.51178085).

References

[1] Yang, Y., Song, X., Zhang, S., Hu, J., Ruan, M., Zeng, D., Luo, H., Wang, J., Wang, Z. "Correlation Analysis and Prediction of the Physical and Mechanical Properties of Coastal Soft Soil in the Jiangdong New District, Haikou, China", Advances in Civil Engineering, 2024(1), 9985210, 2024. https://doi.org/10.1155/2024/9985210

[2] Zou, W.-L., Wang, Z., Yao, Z.-F. "Effect of Dynamic Compaction on Placement of High-Road Embankment", Journal of Performance of Constructed Facilities, 19(4), pp. 316–323, 2005. https://doi.org/10.1061/(ASCE)0887-3828(2005)19:4(316)

[3] Liu, H. L., Ng, C. W.W., Fei, K. "Performance of a Geogrid-Reinforced and Pile-Supported Highway Embankment over Soft Clay: Case Study", Journal of Geotechnical and Geoenvironmental Engineering, 133(12), pp. 1483–1493, 2007. https://doi.org/10.1061/(ASCE)1090-0241(2007)133:12(1483)

[4] Chen, R. P., Xu, Z. Z., Chen, Y. M., Ling, D. S., Zhu, B. "Field Tests on Pile-Supported Embankments over Soft Ground", Journal of Geotechnical and Geoenvironmental Engineering, 136(6), pp. 777–785, 2010. https://doi.org/10.1061/(ASCE)GT.1943-5606.0000295

[5] Nguyen, P.-L. T., Tran, M. H., Tran, T. D., Nguyen, B.-P. "Numerical Analysis of Arching Behavior of Geosynthetic-Reinforced and DCM Column-Supported Embankment with Geosynthetic Characteristics", International Journal of Geosynthetics and Ground Engineering, 9(5), 56, 2023. https://doi.org/10.1007/s40891-023-00474-7

[6] Tong, L., Liu, L., Yu, Q. "Highway construction across heavily mined ground and steep topography in southern China", Bulletin of Engineering Geology and the Environment, 73(1), pp. 43–60, 2014. https://doi.org/10.1007/s10064-013-0503-6

[7] Zhao, G., Yang, Y., Zhang, H., Zhang, G. "A case study integrating field measurements and numerical analysis of high-fill slope stabilized with cast-in-place piles in Yunnan, China", Engineering Geology, 253, pp. 160–170, 2019. https://doi.org/10.1016/j.enggeo.2019.03.005

[8] Illés, Z. "Causes of dike deterioration – environmental and anthropogenic effects", Scientia et Securitas, 3(3), pp. 205–218, 2022. https://doi.org/10.1556/112.2022.00123

[9] Illés, Z., Nagy, L. "Effect of climate change on earthworks of infrastructure: statistical evaluation of the cause of dike pavement cracks", Geoenvironmental Disasters, 9(1), 20, 2022. https://doi.org/10.1186/s40677-022-00221-6

[10] Lawton, E. C., Fragaszy, R. J., Hetherington, M. D. "Review of Wetting-Induced Collapse in Compacted Soil", Journal of Geotechnical Engineering, 118(9), pp. 1376–1394, 1992. https://doi.org/10.1061/(ASCE)0733-9410(1992)118:9(1376)

[11] Cai, Y., Chen, Y., Cao, Z., Ren, C. "A combined method to predict the long-term settlements of roads on soft soil under cyclic traffic loadings", Acta Geotechnica, 13(5), pp. 1215–1226, 2018. https://doi.org/10.1007/s11440-017-0616-3

[12] Hu, H., Hu, S. "公路建设不同阶段软土地基沉降比例研究" (Research on settlement proportion of soft soil foundation for different highway construction stages), Journal of Yangtze River Scientilic Research Institute, 27(6), pp. 35–37, 2010. (in Chinese)

[13] Chai, J.-C., Miura, N. "Traffic-Load-Induced Permanent Deformation of Road on Soft Subsoil", Journal of Geotechnical and Geoenvironmental Engineering, 128(11), pp. 907–916, 2002. https://doi.org/10.1061/(ASCE)1090-0241(2002)128:11(907)

[14] Wang, Z., Li, Y., Shen, R. F. "Correction of soil parameters in calculation of embankment settlement using a BP network back-analysis model", Engineering Geology, 91(2–4), pp. 168–177, 2007. https://doi.org/10.1016/j.enggeo.2007.01.007

[15] Liu, J., Tai, B., Fang, J. "Ground temperature and deformation analysis for an expressway embankment in warm permafrost regions of the Tibet plateau", Permafrost and Periglacial Processes, 30(3), pp. 208–221, 2019. https://doi.org/10.1002/ppp.2007

[16] Shi, X., Huang, J., Su, Q. "Experimental and numerical analyses of lightweight foamed concrete as filler for widening embankment", Construction and Building Materials, 250, 118897, 2020. https://doi.org/10.1016/j.conbuildmat.2020.118897

[17] Zhao, H.-Y., Indraratna, B., Ngo, T. "Numerical simulation of the effect of moving loads on saturated subgrade soil", Computers and Geotechnics, 131, 103930, 2021. https://doi.org/10.1016/j.compgeo.2020.103930

[18] Zhuang, Y., Wang, K. Y. "Finite-element analysis of arching in highway piled embankments subjected to moving vehicle loads", Géotechnique, 68(10), pp. 857–868, 2018. https://doi.org/10.1680/jgeot.16.P.266

[19] Móczár, B. "Construction of a highway embankment on thick marshy ground", Periodica Polytechnica Civil Engineering, 47(2), pp. 199–204, 2003. [online] Available at: https://pp.bme.hu/ci/article/view/615 [Accessed: 24 June 2024]

[20] Stacho, J., Sulovska, M. "Numerical Analysis of Soil Improvement for a Foundation of a Factory Using Stone Columns Made of Different Types of Coarse-grained Materials", Periodica Polytechnica Civil Engineering, 63(3), pp. 795–803, 2019. https://doi.org/10.3311/PPci.13727

[21] Wu, Y., Duan, J., Xu, J., Xu, W. "Failure Mechanism and Structural Optimization of the Primary Support Structure for Expressway Tunnel in Soft Rock: A Case Study", Periodica Polytechnica Civil Engineering, 68(4), pp. 1268–1280, 2024. https://doi.org/10.3311/PPci.36949

[22] Cheng, T., Hu, R., Xu, W., Zhang, Y. "Mechanical Characterizations of Oxidizing Steel Slag Soil and Application", Periodica Polytechnica Civil Engineering, 61(4), pp. 815–823, 2017. https://doi.org/10.3311/PPci.9393

[23] Jia, M., Xu, J., Gao, C., Mu, M., E, G. "Long-Term Cross-Slope Variation in Highways Built on Soft Soil under Coupling Action of Traffic Load and Consolidation", Sustainability, 15(1), 33, 2023. https://doi.org/10.3390/su15010033

[24] Pham, T. A., Dias, D. "3D numerical study of the performance of geosynthetic-reinforced and pile-supported embankments", Soils and Foundations, 61(5), pp. 1319–1342, 2021. https://doi.org/10.1016/j.sandf.2021.07.002

[25] Dassault Systems "ABAQUS, (2018)", [computer program] Available at: https://hpc.dlut.edu.cn/info/1017/1033.htm [Accessed: 17 July 2019]

[26] Dalian University of Technology "SASLEF, (V1.0)", [computer program] Available at: https://github.com/ywtxr/SASLEF-V1.0L [Accessed: 23 March 2025]
[27] Ministry of Transport of the People's Republic of China (MTPRC) "JTG D30-2015 公路路基设计规范"(JTG D30-2015 Specifications for Design of Highway Subgrades), China Communications Press Co., Beijing, China, 2015. (in Chinese)
[28] Duncan, J. M., Chang, C.-Y. "Nonlinear Analysis of Stress and Strain in Soils", Journal of the Soil Mechanics and Foundations Division, 96(5), pp. 1629–1653, 1970. https://doi.org/10.1061/JSFEAQ.0001458
[29] Kondner, R. L. "Hyperbolic Stress-Strain Response: Cohesive Soils", Journal of the Soil Mechanics and Foundations Division, 89(1), pp. 115–143, 1963. https://doi.org/10.1061/JSFEAQ.0000479
[30] Qian, J., Yin, Z. "岩土工程原理與計算" (Geotechnical principles and calculation), Chinese Water Conservancy Hydroelectric Press, Beijing, China, 1996. (in Chinese)
[31] Vámos, M. J., Szendefy, J. "Overconsolidated Stress and Strain Condition of Pavement Layers as a Result of Preloading during Construction", Periodica Polytechnica Civil Engineering, 67(4), pp. 1273–1283, 2023. https://doi.org/10.3311/PPci.22258
[32] da Silva, A. R., de Lima, R. P. "*soilphysics*: An R package to determine soil preconsolidation pressure", Computers & Geosciences, 84, pp. 54–60, 2015. https://doi.org/10.1016/j.cageo.2015.08.008
[33] Bahumdain, A., Tabatabai, H., Titi, H. "Analysis of soil settlement behind bridge abutments", Transportation Geotechnics, 36, 100812, 2022. https://doi.org/10.1016/j.trgeo.2022.100812
[34] Rémai, Z. "Settlement below embankments: factors controlling the depth of the deformation zone", Central European Geology, 57(1), pp. 71–81, 2014. https://doi.org/10.1556/ceugeol.57.2014.1.4
[35] German Institute for Standardisation "DIN 1054 Subsoil - Verification of the safety of earthworks and foundations - Supplementary rules to DIN EN 1997-1", German Institute for Standardisation, Berlin, Germany, 2021. [online] Available at: https://www.en-standard.eu/din-1054-subsoil-verification-of-the-safety-of-earthworks-and-foundations-supplementary-rules-to-din-en-1997-1/ [Accessed: 24 June 2024]
[36] Kempfert, H.-G., Gebreselassie, B. "Excavations and Foundations in Soft Soils", Springer-Verlag Berlin, 2006. ISBN 978-3-642-06944-4 https://doi.org/10.1007/3-540-32895-5
[37] Han, D., Tan, H., Huang, X. M., Hu, H. M. "拼接工况下路基的参数反演与沉降特性" (Parametric inversion and settlement characteristic of subgrade in joint condition), Journal of Traffic and Transportation Engineering, 12(6), pp. 7–12, 2012. (in Chinese) https://doi.org/10.19818/j.cnki.1671-1637.2012.06.002
[38] Wang, X. Z., Chen, M., Wei, H. Z., Meng, Q. S., Yu, K. F. "车辆荷载作用下钙质砂路基的动态响应试验研究" (Experimental study on dynamic response of calcareous sand subgrade under vehicle load), Rock and Soil Mechanics, 39(11), pp. 4093–4101, 2018. (in Chinese) https://doi.org/10.16285/j.rsm.2018.0635
[39] Peirlinck, M., Linka, K., Hurtado, J. A., Kuhl, E. "On automated model discovery and a universal material subroutine for hyperelastic materials", Computer Methods in Applied Mechanics and Engineering, 418, 116534, 2024. https://doi.org/10.1016/j.cma.2023.116534
[40] Lucarini, S., Martínez-Pañeda, E. "UMAT4COMSOL: An Abaqus user material (UMAT) subroutine wrapper for COMSOL", Advances in Engineering Software, 190, 103610, 2024. https://doi.org/10.1016/j.advengsoft.2024.103610
[41] Phutthananon, C., Jongpradist, P., Wonglert, A., Kandavorawong, K., Sanboonsiri, S., Jamsawang, P. "Field and 3D Numerical Investigations of the Performances of Stiffened Deep Cement Mixing Column-Supported Embankments Built on Soft Soil", Arabian Journal for Science and Engineering, 48(4), pp. 5139–5169, 2023. https://doi.org/10.1007/s13369-022-07322-2
[42] Zheng, B., Zhang, J., Qin, Y. "Investigation for the deformation of embankment underlain by warm and ice-rich permafrost", Cold Regions Science and Technology, 60(2), pp. 161–168, 2010. https://doi.org/10.1016/j.coldregions.2009.08.012
[43] Francos, A., Elorza, F. J., Bouraoui, F., Bidoglio, G., Galbiati, L. "Sensitivity analysis of distributed environmental simulation models: understanding the model behaviour in hydrological studies at the catchment scale", Reliability Engineering & System Safety 79(2), pp. 205–218, 2003. https://doi.org/10.1016/S0951-8320(02)00231-4
[44] Zheng, Y., Yue, J., Zhang, P., Duan, J. "Analysis of parameter influence law of waveguide Bragg grating", Optics & Laser Technology, 146, 107576, 2022. https://doi.org/10.1016/j.optlastec.2021.107576
[45] Lenhart, T., Eckhardt, K., Fohrer, N., Frede, H.-G. "Comparison of two different approaches of sensitivity analysis", Physics and Chemistry of the Earth, Parts A/B/C, 27(9–10), pp. 645–654, 2002. https://doi.org/10.1016/S1474-7065(02)00049-9
[46] Wang, X., Wang, X., Yang, G., Zong, Y. "Study on Load Transfer Mechanism of Pile-Supported Embankment Based on Response Surface Method", Applied Sciences, 12(10), 4905, 2022. https://doi.org/10.3390/app12104905
[47] Fei, C. "路基土變形機制試驗與數值模擬研究" (The experimental and numerical simulation study on the mechanism of subgrade soil deformation), MSc thesis, Dalian Maritime University, 2014. (in Chinese)
[48] Zhang, B. "大連路基土改良力學試驗及模型研究" (Studying the mechanics experiment and model of improving subgrade soil in Dalian), MSc thesis, Dalian Maritime University, 2015. (in Chinese)
[49] Farzaneh, O., Iraji, A. "Two-Phase Model for Nonlinear Dynamic Simulation of Reinforced Soil Walls Based on a Modified Pastor-Zienkiewicz-Chan Model for Granular Soil", Journal of Engineering Mechanics, 142(2), 04015072, 2016. https://doi.org/10.1061/(ASCE)EM.1943-7889.0000985